IET Image Processing

*Research Article*

# Complex number-based image quality assessment using singular value decomposition

ISSN 1751-9659
Received on 28th November 2014
Revised on 22nd June 2015
Accepted on 21st July 2015
doi: 10.1049/iet-ipr.2014.0937
www.ietdl.org

*Wang Yong*[1] ✉, *Wang Yuqing*[2], *Zhao Xiaohui*[1]

[1] *College of Communication Engineering, Jilin University, No. 5372, Nanhu Road, Changchun City, Jilin Province 130012, People's Republic of China*

[2] *Key Laboratory of Airborne Optical Imaging and Measurement, Changchun Institute of Optics, Fine Mechanics and Physics, Chinese Academy of Sciences, No. 3888, Dong Nanhu Road, Changchun City, Jilin Province 130033, People's Republic of China*

✉ *E-mail: wang_yong8205@163.com*

**Abstract:** In this study, the combining strategies are considered to be effective tools to improve the performance of the image quality assessment (IQA) metrics. A new metric is proposed to evaluate the quality of test images of combined degradation and individual degradation. The complex numbers are used to describe the image structure in the proposed method. On the basis of that, the properties of the classical IQA method based on singular value decomposition are analysed. The difference between energy visual map and structure visual map is shown. The complex-number-based approach is different from the classical scalar-based techniques, which are insufficient to describe image structure. The proposed C_SVDQ metric can be considered as a vectorial expansion of structure similarity. In the experiments, an extensive comparison between the proposed C_SVDQ and other IQA metrics on image quality database was performed. Both the overall tests and the individual distortion tests show the superiority of this new approach in IQA.

## 1 Introduction

In many applications of image processing, the objective image quality assessment (IQA) plays important roles. The objective IQA metrics are necessary to be developed to automatically measure image quality. For the complex task of objectively assessing perceived image quality, many approaches, therefore, rely on the hypothesis to which image distortions of the visual system of human (HVS) is particularly sensitive. However, in practice, it is hard to distinguish the complicated image distortions. They can be discerned only when the specific processing method is known or the distorted images are generated by predefined mathematical models. In most of the applications, the simple predefined distortions, such as the blur and noise distortion, are only used in some experiments in order to evaluate the behaviours of the IQA metrics. Generally, there are three main classes of objective IQA metrics. The most widely used IQA methods are full reference metrics. They utilise the similarity between the distorted image and its corresponding reference image. Although the full reference metrics require the availability of the reference image, they are often used as important tools for experiments of image processing algorithms. No reference metrics are more sensible as far as the process of image perception because the quality prediction of the HVS in real world is based on the output image only. Owing to our limited knowledge on the HVS, it is a challenging work to design no reference IQA metrics. On the basis of the direct estimation on a specific type of distortion the no reference metrics are proposed in [1–6], such as blurred images, noise distorted images and some types of compressed images. However, as mentioned previously, since the complicated distortions in real world are hard to be classified into some separated ones, the no reference IQA metrics may have some uncertain behaviour when they are performed in the applications. The reduced reference IQA metrics also need the availability of a reference image, but the information transmitted from reference images to output images is simpler than the full reference IQA metrics. In this paper, we mainly discuss the full reference IQA methods, where the reference images can be obtained when evaluating the distorted images.

Since the sensible subjective IQA metrics cannot be easily implemented in real-time and automated systems, the robust objective IQA metrics are necessary to be designed to automatically evaluate image visual quality. It is known to all that the mean squared error (MSE) method is widely used in many fields of image processing, but its performance is poorly correlated with the perceived image quality. Only in some simple applications, better performance can be achieved when they are applied to the assessment of the non-structured distortions [7]. The peak signal-to-noise ratio (PSNR) metric has the same behaviour. Thus, many IQA metrics are designed using the HVS models. In these models, the HVS sensitivities to different types of visual signals are emphasised, such as the contrast and the frequency properties in an image. The structure-based methods, such as the structural similarity index (SSIM) [8, 9], are inspired by the structure properties in an image, they are proposed to reflect more complicated distributions in an image. In SSIM, the HVS is considered as highly sensitive to the structural information in an image. The SSIM outputs overall objective assessment results by calculating the average of SSIM values for all the sliding blocks in an image. The performance of our method is better than the traditional full reference methods. In the last few decades, considerable progress in HVS modelling has been made, and some successful models are widely used in many IQA methods [10–12]. They assess the image quality by modelling the behaviours of the HVS. In fact, it is an enormous task to describe all the HVS characteristics and integrate them into a fine mathematical model. Therefore, many of the simple HVS-based metrics do not show any performance improvement in comparison with the traditional methods in most of the applications.

The general belief is that the HVS possesses image structure sensitive property that plays an important role in image perception. To further improve the performance of the IQA metrics, some complicated transforms are used in some applications [13–16]. The multiscale geometric analysis metric uses mathematical model to mimic the multichannel property of the HVS [14]. These solutions are attractive since they provide more effective representation for the structural information. Recently, many metrics have been proposed to reflect image quality visually. Shnayderman *et al.* [17] introduced an effective IQA algorithm called 'MSVD'. The grey-scale images are divided into some blocks and the singular value decomposition (SVD) transform is performed on the blocks. Then the singular value block is produced by this method.

The calculation of pixel errors is considered as an important basis in full reference metrics. SSIM is a widely used IQA metric that has many versions. Many researchers choose to expand the work of SSIM in order to improve the performance of their models [18–20]. In the spatial domain, the task can be performed by some statistical models of locally normalised coefficients, such as the gradient map and local variance distribution map. The gradient map can reflect the HVS-sensitive information contained in an image as changes in pixel values. The gradient-based IQA approaches were proved to perform better than the pixel-to-pixel approaches, such as the gradient structural similarity index (GSSIM) [21, 22]. In addition, it is assumed in [23] that there is a great amount of HVS-sensitive information in the local variance distribution of an image. On the basis of that, the quality assessment index based on local variance (QILV) was proposed and proved to be highly sensitive to the changes of image detail information [23]. The QILV can be considered as a general framework, which can reflect the change of structural information in an image.

From the experimental results of the previous work, it can be found that many of the state-of-the-art IQA measures have some uncertain behaviours. For instance, few of them can give the best performance for all the specific types of artefacts in the LIVE database [24]. The IQA metrics aim to correlate well with the perceived quality of the HVS in all the possible types of image degradation. However, with regard to different types of distortion, the perceiving process of human is different. Therefore, due to our limited knowledge on the HVS, few IQA metrics can give the best result for all the possible types of distortion. In fact, the perceived image quality should be considered as a well-balanced combination of many types of the properties of HVS. However, the artefacts in the distorted images can hardly be decomposed into some simple types of distortion, such as noise or blur. Therefore, the image structure description method simply defined by some geometric analysis or spatial pixel data using predefined transform functions cannot give a comprehensive interpretation to the image distortion. In [25, 26] some metrological considerations on the IQA metrics are given. They aim to give a solution for uncertainty evaluation in image structure and measurement modelling for IQA metrics. The vector root mean squared error (VRMSE) method provides a new framework for IQA [25]. It can measure the image quality by describing the structural information using vector, such as detail preservation and noise cancellation. The vector-based methods can also output numerical evaluation results. However, the VRMSE is only used in the evaluation for the distorted images corrupted by Gaussian noise.

To better correlate with the human subjective tests, we proposed a combined IQA method using complex numbers. The images degraded by noise distortion, blur, or a combination of both can be evaluated or measured by the method. More importantly, the performance of our new IQA method on all the types of degradation is more sensible than the other state-of-the-art IQA methods. In our study, the complex number is applied to represent image structure. The proposed method is different from the VRMSE approach. The complex matrix is considered as a combination of the HVS-sensitive information and some other unknown structural information. Owing to the limited knowledge on the HVS, our approach is based on the hypothesis that the image structural information cannot be described by a single model. The proposed approach is different from the existing vector-based approaches and provides a complex matrix that can be used in many fields of image processing. The complex numbers are used to construct complicated matrices for the test images. Then the SVD is performed on the matrices. The standard deviation of the singular values corresponding to each block in the matrices is considered as the representation of its structural properties. Then the numerical result is obtained by calculating the median value of the distortion map for the test images.

The rest of this paper is organised as follows. Section 2 discusses the complex number representation for the image structure. In Section 3, the traditional MSVD approach is analysed, then another distortion map generating approach is given which can be considered as an improvement for this method. We then give some experimental results in Section 4 and conclusion is summarised in Section 5.

## 2 Complex number-based image structure representation

In practice, there are various forms of distortion that may affect image structure, but it is impossible to describe all the artefacts using fine mathematical models. Most of the IQA models aim to output numerical results. The traditional calculation form meets the users' needs in most of the applications. The vector-based approach for full reference IQA [25] was proposed in order to study the behaviour of detailed preservation and noise cancellation in an image. It was applied to evaluate the distorted images with additive noise, such as the Gaussian and impulse noise. In fact, the perceived quality of human observers can be considered as an integration of some HVS-sensitive attributes, it is different from the software quality assessment which inspired the VRMSE approach [25].

The framework of many IQA metrics can be summarised as follows. First, the local quality or distortion should be measured by mathematical tools. Second, pooling is performed on the results. The pooling stage is an important stage in the process, which needs reliable computational models, but significant progress is usually made in the first stage. Due to the lack of theoretical principles, the pooling process is always done in simple ways [16]. The overall output of the VRMSE is the pooling result of the vector-based approach. However, this process in HVS is much more different from the simple Minkowski pooling. The simple Minkowski polling process seems to be quantitatively manageable, but the results are not qualitatively sensible. Clearly, an image quality measurement based on the vector method that aims at inspecting the behaviour of image distortion should be able to evaluate the image features separately. Nevertheless, it is different from the traditional quantified method that the vector approach provides a new image quality measurement tool. Many properties of image quality can be described by the vectors. For the purpose of measurement, some useful information that is necessary for support decision can be provided by the vector-based measurement.

The visual inspection of human eyes is more sensitive to some types of structural information in an image. The concept of detail information is often used to describe these types of structural information, but it is obviously too extensive and complicated for modelling. To describe the structural change in a distorted image, a vector tool is used to describe the combination of the detail information and other unknown information corresponding to the pixel at location$(x, y)$ of an image. The vector is defined as

$$\boldsymbol{I}_V(x, y) = \left[I_S(x, y), I_P(x, y)\right] \qquad (1)$$

where $I_S(x, y)$ and $I_P(x, y)$ denote the HVS-sensitive information and other unknown structural information described by the local pixel distribution at location $(x, y)$ of image $I$, respectively. In this study, the vector is considered as a combination tool to represent structural information. When we perform the measurement of the difference between two vectors a need for a combined IQA method arose. Since the goal of the proposed approach is to obtain a quantised overall measure, a simple implementation method for vector measure is to resort the complex number. Then, the vector component $\boldsymbol{I}_V(x, y)$ in (1) can be defined by complex number as


*IET Image Process.*, 2016, Vol. 10, Iss. 2, pp. 113–120

follows:

$$\boldsymbol{I}_V(x, y) = I_S(x, y) + I_P(x, y) \times i \tag{2}$$

where $\boldsymbol{I}_V(x, y)$ is the complex number corresponding to the pixel at location $(x, y)$ of image $I$. Respectively, $I_S(x, y)$ and $I_P(x, y)$ represent the detail information and other unknown information described by pixel distribution as what is discussed previously. Then the combination of the HVS-sensitive information and the extensive pixel distribution information in an image can be implemented using the complex matrix composed of the components defined in (2).

Application of the proposed approach is restricted within the grey-scale image. The calculation for colour image can be performed on its luminance layer, which can be obtained by separating the luminance information from the input image.

In this study, the performance of our IQA method is highly relevant to the representation of the image detail information. The local variance distribution is proved to be a very effective tool to describe the image structure by Aja-Fernandez *et al.* [23]. For the sliding block $Ix, y$ in image $I$ that contains $L$ pixels, namely $\eta_p$, the local variance is expressed as follows:

$$\mathrm{Var}(Ix, y) = E\{(Ix, y - \bar{I}x, y)^2\} \tag{3}$$

where $\bar{I}x, y$ is defined as

$$\bar{I}x, y = \frac{1}{L}\sum_{p=1}^{L} \eta_p \tag{4}$$

$\bar{I}x, y$ is the mean value of the pixels in the image. Then the local variance distribution is

$$\mathrm{Var}(Ix, y) = \frac{1}{L}\sum_{p=1}^{L} (\eta_p - \bar{I}x, y)^2 \tag{5}$$

$\mathrm{Var}(Ix, y)$ and $\bar{I}x, y$ are estimated using a Gaussian weighed neighbourhood centred on the pixel $(x, y)$ in order to overcome the 'blocking' artefacts in the SSIM visual map [9]. Since the SSIM visual map is not used in this work, (4) and (5) are directly used to calculate these parameters.

When the local variance distribution of a grey-scale image is estimated by (5), it can be used as a description for the image structure [23]. Although the results from experiments show that the QILV index cannot provide a comprehensive description for the image structure, it was proved to be highly relevant to the changes of image detail information. The local variance distribution can be considered as a claimed solution for the representation of $I_S(x, y)$ in (2). Then the term $\boldsymbol{I}_V(x, y)$ in (2) can be expressed as follows:

$$\boldsymbol{I}_V(x, y) = \mathrm{Var}(Ix, y) + P(x, y) \times i \tag{6}$$

where $P(x, y)$ is the value. According to (6), a complex matrix can be generated to represent the image structure. Our hypothesis is that the distortion in an image changes the characteristic statistical properties of its corresponding complex matrix, and predicting the amount and type of these changes will make it possible to perform the task of IQA. The utilisation of complex numbers makes the process of image quality measurement more sensible. Although the complex matrix contains HVS-sensitive structural information, it is not a visual map for perceiving. Complicated properties of the complex matrix should be analysed by further decomposition.

## 3 Distortion map and numerical measure

SVD is an effective tool in the field of image processing. The singular values were proved to be reasonably effective for the image texture classification [27]. A real or complex matrix $\boldsymbol{A}$ with rank $r$ can be decomposed into a product of three matrices as

$$\boldsymbol{A} = U\begin{pmatrix} \boldsymbol{\Sigma}_r & 0 \\ 0 & 0 \end{pmatrix}V^{\triangleleft} \tag{7}$$

The real diagonal matrix is denoted by $\boldsymbol{\Sigma}_r$. There are $r$ non-null entries $s_i\ (1 \le i \le r)$ on its diagonal. $\triangleleft$ denotes the conjugate-transposition operator.

Let $\boldsymbol{x}$ be the singular value vector

$$\boldsymbol{x} = (s_1, s_2, \ldots, s_r, 0, \ldots, 0)^{\mathrm{T}} \tag{8}$$

where T is the transpose operator. The distance between the two vectors can be calculated to generate the distortion map [17]. The value of each pixel in the visual map of distortion can be obtained by the function defined as

$$D_k = \mathrm{Sqrt}\left[\sum_{i=1}^{n} (s_i - \hat{s}_i)^2\right] \tag{9}$$

It was pointed out by Narwaria and Lin [19] that each $s_i$ denotes a part of the matrix energy but not the image structure. The singular value vector is not highly relevant to the structural information. In other words, the change of $\boldsymbol{x}$ reflects the change of matrix energy which should be discussed within the field of information theory but not the field of human perception. In this paper, the SVD-based approach is still used to evaluate image quality, but it is implemented based on some improved mechanisms. They can be summarised as follows:

First, as introduced in the previous sections, the SVD is performed on the complex matrix composed of the components defined in (6). The singular value vector can be considered as the representation for the energy of the complex matrix. Since more HVS-sensitive information is contained in the complex matrix, its singular value vector is more relevant to the image structure. Therefore, the importance of the singular value vector for the image structural information is improved comparing with that of the simple real matrix. Then, the improved consistency of the HVS with the singular value vector is achieved by using the proposed complex matrix.

Second, as the range of the singular values corresponding to a given image block is related to its activity pixel level, all the components in the singular value vector should be used in the graphical measure [17]. In this paper, another approach is used to perform the task. The standard deviation of the singular values corresponding to each block is calculated as an estimation of its structure change. It is defined as

$$D_k = \sqrt{\frac{\sum_{i=1}^{r} (s_i - \bar{s})^2}{r - 1}} \tag{10}$$

Fig. 1 gives an example to show the values of standard deviation corresponding to some of the image blocks.

It can be seen obviously from the results in Fig. 1 that different blocks have different activity levels and different standard deviations. The lower the activity level is, the larger the standard deviation is. In the visual perception point of view, the block with highest activity level is block A, then the proposed method gives the smallest standard deviation to it. Furthermore, the proposed method also distinguished the activity level in blocks B and C correctly.

The distortion map is obtained by calculating the standard deviation of the blocks corresponding to the test images

$$\mathrm{DS}_k = \left|D_k - \hat{D}_k\right| \tag{11}$$

where $D_k$ and $\hat{D}_k$ denote the standard deviations corresponding to the

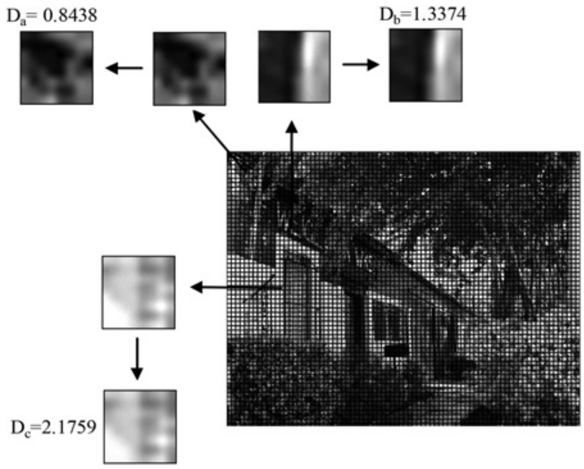


**Fig. 1** *Standard deviation of singular values in different blocks (luminance layer of the colour image)*

*k*th block in the test images, respectively. The generating approach of the distortion map proposed in our study is different from the traditional method [17]. It calculates the distance between the standard deviation of singular values, but not the distance between two singular value vectors. To visualise the difference, some distortion maps are generated using the MSVD method in [17] and the proposed method for the two distorted images derived from the same reference image. The comparison results are given in Fig. 2.

To observe the distortion maps clearly, they were enlarged and the value of the pixels in the distortion map was mapped to the range 0–255. From the visual perception point of view, the observers can intuitively perceive that the different distortion maps derive from different types of distortion. The accurate numerical results need further processing on the distortion maps. It can be seen from the distortion maps in Fig. 2 that the MSVD method generates almost the similar structure for the noise distorted image and the blurred image. For instance, Fig. 2*d* is almost as visible as Fig. 2*e*. The contours can be seen clearly in Figs. 2*d* and *e* whereas the proposed method distinguishes them distinctly. The difference between the distortion types can be discerned from the perceived difference between Figs. 2*f* and *g*. Therefore, the proposed IQA method performs better than that of the MSVD method in terms of the visual perception of the distortion maps in Fig. 2.

Calculation of the proposed numerical measure C_SVDQ is also derived from the distortion map. It is defined as

$$\text{C\_SVDQ} = \frac{\sum_{i=1}^{(N/k)\times(M/k)} \left|\text{DS}_i - \text{DS}_{\text{mid}}\right|}{(N/k)\times(M/k)} \tag{12}$$

where $k$ denotes the block size, $\text{DS}_{\text{mid}}$ denotes the median value of $\text{DS}_i$. Fig. 3 is the framework diagram of the proposed C_SVDQ method.

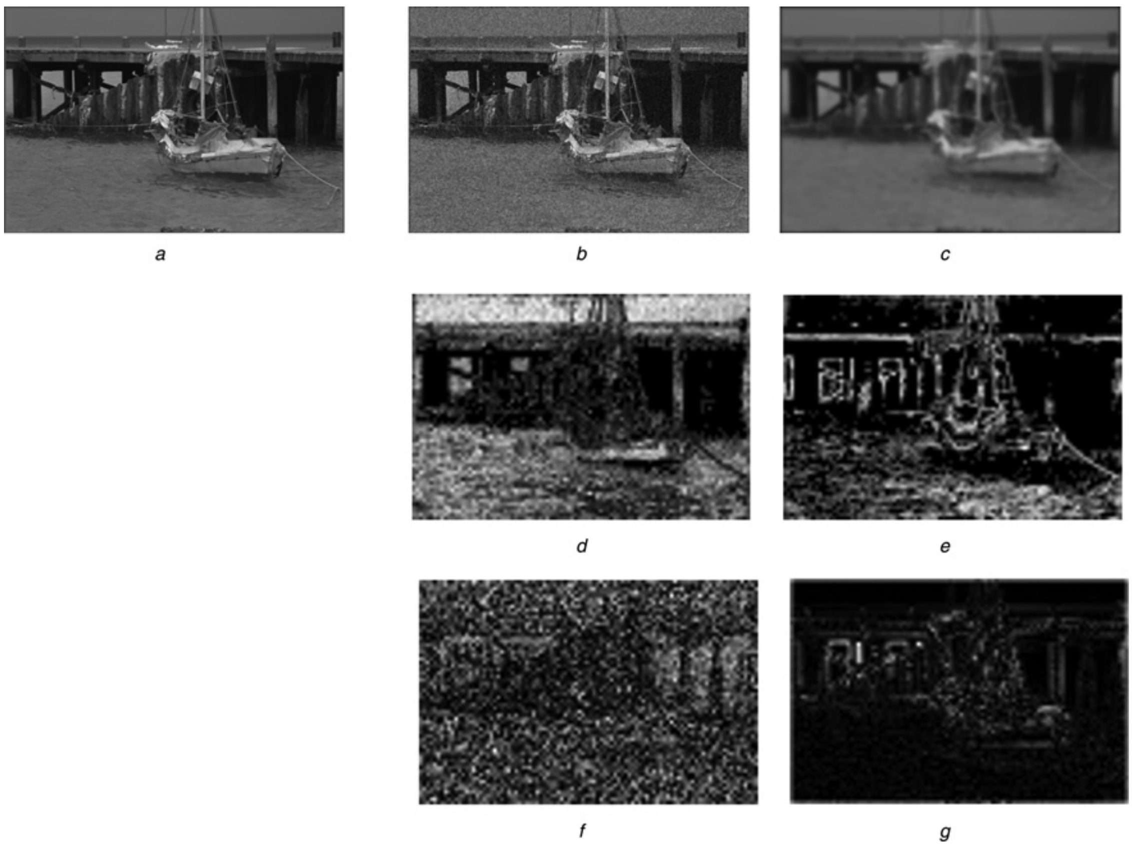


**Fig. 2** *Comparison of distortion maps*

*a* Reference image
*b* Noise distorted image
*c* Blurred image
*d* Distortion map for Fig. 2*b* obtained by MSVD [17]
*e* Distortion map for Fig. 2*c* obtained by MSVD [17]
*f* Distortion map for Fig. 2*b* obtained by the proposed method
*g* Distortion map for Fig. 2*c* obtained by the proposed method

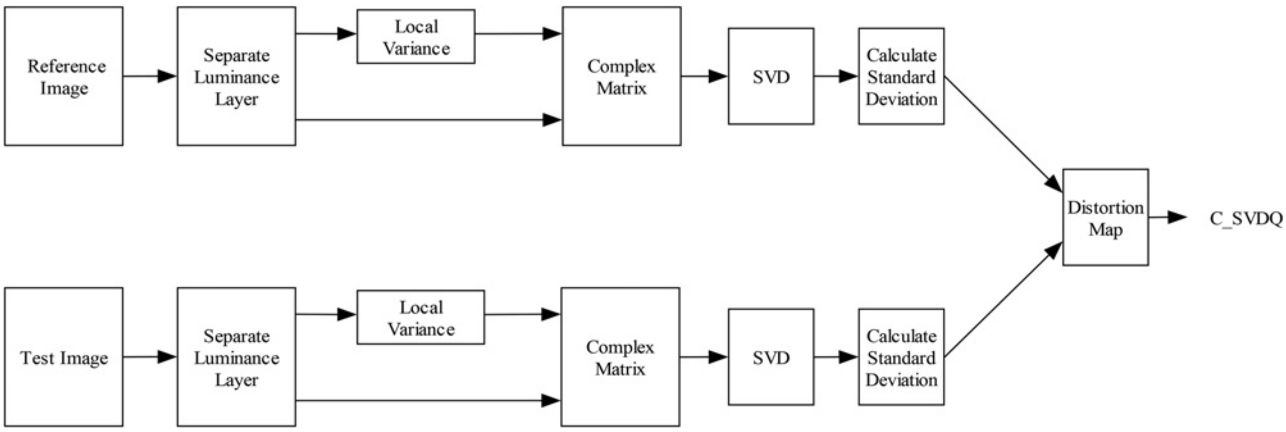


**Fig. 3** *Framework diagram of the proposed C_SVDQ method*

## 4 Experimental results

Objective IQA aims to output measure results which have good correlation with the HVS. The prediction is an automatical and robust process. The most widely used way to demonstrate validity of IQA metrics is to evaluate their consistency with the HVS by using the test image database. To inspect the performance of the C_SVDQ index, we use the LIVE test database [24]. It contains 779 distorted images. They are all from the 29 reference images in the same database. There are five different distortion categories in the database. They are compression database (JPEG2000 and JPEG compressed images), distorted images with additive Gaussian noise, blurred images and a Rayleigh fast fading channel distortion data sets. The difference mean opinion score (DMOS) value related to each test image represents its theoretical subjective quality, in terms of in-lab test. To demonstrate the general effectivity of the proposed C_SVDQ method, all the distorted images in the five data sets were used for testing only. Testing and comparison between C_SVDQ and other IQA methods were done on the LIVE database. The process can show the superiority of the C_SVDQ over other state-of-the-art IQA methods. We compared our new C_SVDQ method, against common IQA methods, such as MSE, PSNR, MSSIM [9], MSVD [17], and QILV [23].

On the basis of that, two special methods were also evaluated in these experiments. They were named C_MSVD and S_MSVD. C_MSVD was calculated using the complex representation proposed in this paper, but its distortion map was generated using the MSVD method [17]. S_MSVD is different from MSVD in that its distortion map was obtained using the method as that in C_SVDQ. To evaluate how well the IQA predictions agree with human perception, the correlation between its prediction results and subjective perception must be computed. The correlation of all the IQA metrics in the experiment was calculated after compensating for the non-linear mapping between the two types of scores. A logistic function with three parameters recommended by video quality experts group [28] was used to perform the non-linear regression for all the metrics. It is defined as

$$\mathrm{DMOS}_q = \frac{b_1}{1 + \exp(-b_2 \times (\mathrm{C\_SVDQ} - b_3))} \tag{13}$$

where $b_1$, $b_2$, and $b_3$ can be obtained numerically using a non-linear regression toolbox. In our method, the complex matrix is divided into $8 \times 8$ blocks. Then the SVD transform is performed on each block to produce a singular value block. We have two reasons to define the block size. In the first instance, the same block size is defined and widely used in JPEG compressed images and other image processing applications. In the next place, many IQA metrics, such as the MSVD and SSIM also use a sliding window size of $8 \times 8$. Therefore, we define the block size not only for the purpose of comparison but also under the consideration of rationality of the parameters. Fig. 4 shows the results of logistic curves fitted for all the eight IQA metrics.

Fig. 4 gives the scatter distributions for the eight IQA indices on the 779 distorted images in LIVE database. The curves show the subjective DMOS scores versus the predicted scores by human visual system. The curves were generated by implementing non-linear fitting as defined in (13). From Fig. 4, we can see that the measurement results give a demonstration that the correlation between the DMOS scores and the scores of the proposed C_SVDQ method are better than other methods. The further investigation on the consistency and behaviours of the proposed method acquires more quantised metrics. Then these competing IQA metrics are evaluated by three performance metrics. They are shown in the following, where $x$ and $y$ denote input signals, respectively.

- *Kendall's rank correlation coefficient (KRCC)*: The metric can be shortened to KRCC. It is a correlation metric and can be expressed as

$$\mathrm{KRCC} = \frac{N_{\mathrm{c}} - N_{\mathrm{d}}}{(1/2)N(N-1)} \tag{14}$$

The discordant and concordant signal pairs in the input signals are denoted by $N_{\mathrm{d}}$ and $N_{\mathrm{c}}$. The metric is used to evaluate the prediction monotonicity.

- *Spearman's rank correlation coefficient (SRCC)*: The metric can be shortened to SRCC. It is expressed as

$$\mathrm{SRCC} = 1 - \frac{6\sum d_i^2}{n^2(n^2-1)} \tag{15}$$

The difference between the $i$th input signals $x_i$ and $y_i$ is expressed by $d_i = x_i - y_i$. It can be also used to evaluate the prediction monotonicity.

- *Root mean square error (RMSE)*: The metric can be shortened to RMSE. It is expressed as

$$\mathrm{RMSE}(x, y) = \sqrt{\frac{1}{n}\sum (x-y)^2} \tag{16}$$

RMSE is used to evaluate the prediction accuracy.

In the first place, all the 779 distorted images were used to perform the task of IQA. The reference images are excluded in our tests in order to avoid several problems in implementing the metrics. Above all, when the reference image is same as the test image some of the IQA metrics may have difficulties in outputting results. For instance, some of the IQA metrics may have infinite

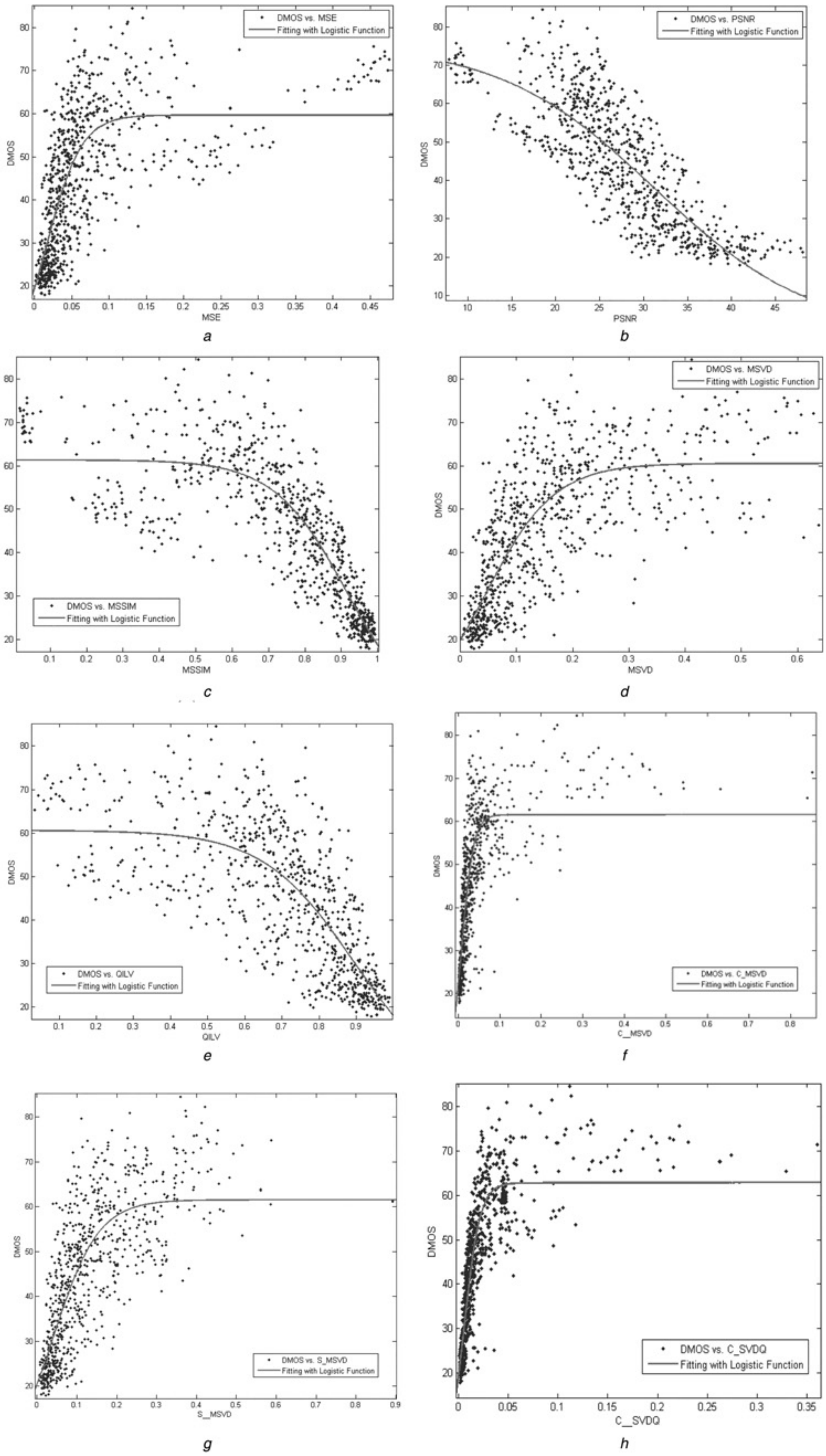


**Fig. 4** *Assessment method comparison*

*a* MSE
*b* PSNR
*c* MSSIM
*d* MSVD
*e* QILV
*f* C_MSVD
*g* S_MSVD
*h* Proposed C_SVDQ

**Table 1** Performance comparison of IQA metrics for the 779 distorted images

| | MSE | PSNR | MSSIM | MSVD | QILV | C_MSVD | S_MSVD | C_SVDQ |
|---|---|---|---|---|---|---|---|---|
| KRCC | 0.5328 | 0.6171 | 0.6549 | 0.5713 | 0.5536 | 0.6472 | 0.5839 | 0.7063 |
| SRCC | 0.7347 | 0.8197 | 0.8510 | 0.7737 | 0.7582 | 0.8399 | 0.7874 | **0.8908** |
| RMSE | 10.94 | 9.379 | 8.152 | 10.25 | 10.43 | 9.079 | 10.05 | **7.549** |

**Table 2** Performance comparison of IQA metrics on the individual data sets

| | | MSE | PSNR | MSSIM | MSVD | QILV | C_SVDQ |
|---|---|---|---|---|---|---|---|
| JPEG2000 | KRCC | 0.6016 | 0.7037 | 0.7633 | 0.6726 | 0.7426 | 0.7984 |
| | SRCC | 0.8027 | 0.8898 | 0.9317 | 0.8621 | 0.9177 | 0.9481 |
| | RMSE | 9.709 | 7.519 | 5.754 | 8.289 | 6.429 | 5.003 |
| JPEG | KRCC | 0.5817 | 0.6355 | 0.7145 | 0.6523 | 0.7024 | 0.7179 |
| | SRCC | 0.7911 | 0.8409 | **0.9028** | 0.8540 | 0.8959 | 0.9015 |
| | RMSE | 9.894 | 8.5 | 6.02 | 8.085 | 6.738 | 5.658 |
| Gaussian noise | KRCC | 0.8061 | **0.8941** | 0.8362 | 0.6588 | 0.8193 | 0.8496 |
| | SRCC | 0.9490 | **0.9853** | 0.9629 | 0.8450 | 0.9581 | 0.9694 |
| | RMSE | 5.126 | **2.742** | 3.976 | 8.404 | 6.035 | 5.48 |
| Gaussian blur | KRCC | 0.5238 | 0.5847 | 0.7136 | 0.5847 | 0.5879 | 0.7577 |
| | SRCC | 0.7104 | 0.7816 | 0.8942 | 0.7721 | 0.7794 | 0.9222 |
| | RMSE | 10.98 | 9.878 | 7.722 | 9.932 | 10.2 | 6.201 |
| fast fading | KRCC | 0.6435 | 0.7067 | **0.7814** | 0.7529 | 0.7580 | 0.7176 |
| | SRCC | 0.8425 | 0.8903 | **0.9411** | 0.9190 | 0.9263 | 0.8768 |
| | RMSE | 9.039 | 7.674 | **5.787** | 6.559 | 6.085 | 8.488 |

value, such as PSNR. Then the non-linear regression can hardly be performed. Additionally, since it is assumed that all the original images have perfect quality, the natural relative ranks between them cannot be computed. There are considerable ambiguities in the computing of SRCC and KRCC metrics [16]. Finally, it is merely an assumption that the quality of the reference images is perfect in terms of their DMOS value. Due to the complicated properties of the HVS, further analysis is necessary for this theoretical conclusion.

Theoretically, with the performance improvement of the objective IQA metrics, their SRCC and KRCC values should be higher, while the RMSE values should be lower. Table 1 shows our performance comparison for the eight IQA measures of the 779 distorted images in the LIVE database. The table provides an investigation for the overall performance of the IQA measures under comparison. In our experiments, the IQA metric achieving the best performance is highlighted in boldface. It can be seen from the table clearly that our proposed C_SVDQ outperforms all the other IQA metrics in our comparison experiments. This confirms our assumption that C_SVDQ is an effective tool to measure the combined degradation. Moreover, it can be seen that the two special methods C_MSVD and S_MSVD perform better than MSVD, though they are not as good as C_SVDQ. Therefore, it can be considered as a demonstration that the two optimised mechanisms in our study improve the performance of the conventional SVD-based IQA methods.

**Table 3** Variance of numerical performance measure of the IQA methods for the individual distortion type

| | MSE | PSNR | MSSIM | MSVD | QILV | C_SVDQ |
|---|---|---|---|---|---|---|
| KRCC | 0.0114 | 0.0138 | **0.0026** | 0.0082 | 0.0067 | 0.0032 |
| SRCC | 0.0076 | 0.0056 | **0.0008** | 0.0090 | 0.0053 | 0.0013 |
| RMSE | 5.0548 | 7.2606 | 1.7646 | **1.4352** | 3.0889 | 1.8685 |

The behaviours of the proposed C_SVDQ method should be deeply investigated by individual types of distortion. The five individual data sets in the LIVE database are used in our tests in order to evaluate its different sensitivity to different types of distortion. Table 2 shows the measurement results.

From the experimental results summarised in Table 2, we can see clearly that the proposed method achieves the best results on most of the individual data sets in the LIVE database. Obviously, the C_SVDQ has better performance in dealing with the distortions of JPEG2000 compressed images and Gaussian blurred images. In addition, it produced the highest KRCC value and the lowest RMSE value for the compressed images of JPEG, and the SRCC value of C_SVDQ is very close to the highest value. The PSNR metric performs much better than the other IQA indices for the test of Gaussian noise distorted images, but the C_SVDQ and PSNR have comparable performance for the metric of KRCC and SRCC. For the fast fading images, the MSSIM outperforms the

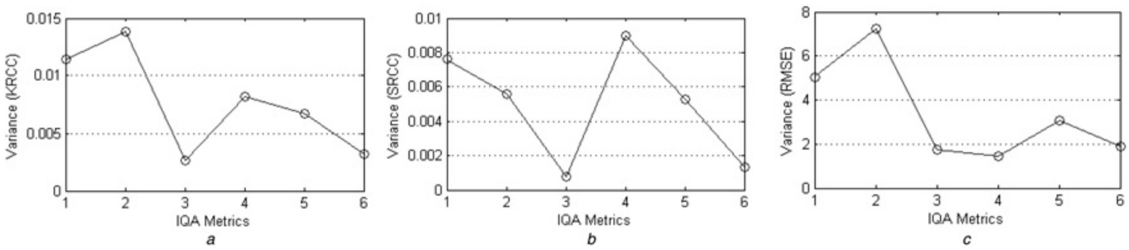


**Fig. 5** *Variance of the assessment results for the individual distortion types, the numbers one to six in the X-axis denote MSE, PSNR, MSSIM, MSVD, QILV, and C_SVDQ, respectively*

*a* Variance of their KRCC values
*b* Variance of their SRCC values
*c* Variance of their RMSE values

other IQA metrics used in comparison experiments. Nevertheless, for most of the distortion types, the behaviours of the C_SVDQ are better than those of the other IQA metrics. From Fig. 1 and Table 2, one can see that the correlation between the objective results given by C_SVDQ and the subjective results are much better than the other methods.

In Table 3, the variance values of the numerical performance measure for the IQA metrics to these distorted images with specific types of distortion in Table 2 for KRCC, SRCC and RMSE are shown. It is a rather simple method to measure the fluctuation of their sensitivity to different distortion types. The IQA metrics with lower variance values have more uniform sensitivity to different distortion types. Obviously, the MSSIM has the lowest variance for KRCC and SRCC, and the MSVD has the lowest variance for RMSE. However, the variance of the proposed C_SVDQ method is very close to the lowest value, which can be seen more clearly in Fig. 5.

## 5 Conclusions

The combining strategies are considered as effective tools to improve the performance of the IQA metrics in this paper. Aiming at finding the appropriate strategies for IQA algorithms, we studied the vector-based IQA metrics. We use the complex numbers to describe image structure. The proposed method can be considered as an extension of classical vector-based methods. Furthermore, some metrological considerations on the IQA metrics are given. They aim at uncertainty evaluation in image structure and measurement modelling for IQA metrics. The standard deviation of singular values corresponding to each block in the complex matrix was used to represent its structure change. Then the graphical measure and numerical measure were implemented. The behaviours of the proposed method were evaluated using the distorted images in the LIVE database. For the purpose of comparison the proposed strategies and some other conventional IQA methods are investigated in the experiments. The experimental results show that this novel combining strategy causes significant performance improvement of conventional MSVD IQA algorithms. The proposed C_SVDQ algorithm achieves the best performance in the overall test. For the applications of images corrupted by individual distortion types, the proposed method also achieves the best performance.

It can be easily seen from the theoretical analysis and experimental results that the proposed C_SVDQ method is an attractive IQA method. The two optimised mechanisms applied in C_SVDQ improve the performance of the traditional SVD-based IQA methods. The proposed method aims to extend the traditional image structure representation methods which are widely used in the field of IQA. The new framework is not only a combining method, but also a new description method to evaluate image quality. Since the proposed C_SVDQ method is restricted within grey-scale images, improvement on this work will aim to use colour information to perform the task.

## 6 Acknowledgment

This work was supported by the National Natural Science Foundation of China (no. 61201368)

## 7 References

1 Shen, J., Li, Q., Erlebacher, G.: 'Hybrid no-reference natural image quality assessment of noisy, blurry, JPEG2000, and JPEG images', *IEEE Trans. Image Process.*, 2011, **20**, (8), pp. 2089–2098
2 Parvez Sazzad, Z.M., Kawayoke, Y.,, Horita, Y.: 'No reference image quality assessment for JPEG2000 based on spatial features', *Signal Process., Image Commun.*, 2008, **23**, (4), pp. 257–268
3 Zhang, J., Le, T.M.: 'A new no-reference quality metric for JPEG2000 images', *IEEE Trans. Consum. Electron.*, 2010, **56**, (2), pp. 743–750
4 Venkatesh Babu, R., Suresh, S., Perkisc, A.: 'No-reference JPEG-image quality assessment using GAP-RBF', *Signal Process.*, 2007, **87**, (6), pp. 1493–1503
5 Wang, Z., Sheikh, H.R., Bovik, A.C.: 'No-reference perceptual quality assessment of JPEG compressed images'. IEEE Int. Conf. on Image Processing, Rochester, NY, USA, 2002, vol. 1, pp. I-477–I-480
6 Suresh, S., Venkatesh Babu, R., Kim, H.J.: 'No-reference image quality assessment using modified extreme learning machine classifier', *Appl. Soft Comput.*, 2009, **9**, (2), pp. 541–552
7 Ginesu, G., Massidda, F., Giusto, D.D.: 'A multi-factors approach for image quality assessment based on a human visual system model', *Signal Process., Image Commun.*, 2006, **21**, (4), pp. 316–333
8 Wang, Z., Bovik, A.C.: 'A universal image quality index', *IEEE Signal Process. Lett.*, 2002, **9**, (3), pp. 181–184
9 Wang, Z., Bovik, A.C., Sheikh, H.R., *et al.*: 'Image quality assessment: from error visibility to structural similarity', *IEEE Trans. Image Process.*, 2004, **13**, (4), pp. 600–612
10 Westen, S.J.P., Lagendijk, R.L., Biemond, J.: 'Perceptual image quality based on a multiple channel HVS model'. IEEE Int. Conf. on Acoustics, Speech, and Signal Processing, Detroit, MI, USA, 1995, vol. 4, pp. 2351–2354.
11 Maloigne, F., Larabi, C., Bringier, M.C., *et al.*: 'Spatio-temporal characteristics of the human color perception for digital quality assessment'. Int. Symp. on Signals, Circuits and Systems, New York, 2005, vol. 1, pp. 203–206
12 Barni, M., Bartolin, F., Rosa, A.D.: 'HVS modelling for quality evaluation of art images'. Fourteenth Int. Conf. on Digital Signal Processing, Santorini, Greece, 2002, vol. 1, pp. 91–94
13 Kim, D.O., Park, R.H.: 'Evaluation of image quality using dual-tree complex wavelet transform and compressive sensing', *Electron. Lett.*, 2010, **46**, (7), pp. 494–495
14 Gao, X.B., Lu, W., Tao, D.H.: 'Image quality assessment based on multiscale geometric analysis', *IEEE Trans. Image Process.*, 2009, **18**, (7), pp. 1409–1423
15 Beghdadi, A., Pesquest, P.B.: 'A new image distortion measure based on wavelet decomposition'. Seventh Int. Symp. on Signal Processing and its Applications, Paris, France, 2003, pp. 485–488
16 Wang, Z., Li, Q.: 'Information content weighting for perceptual image quality assessment', *IEEE Trans. Image Process.*, 2011, **20**, (5), pp. 1185–1198
17 Shnayderman, A., Gusev, A., Eskicioglu, A.M.: 'An SVD-based grayscale image quality measure for local and global assessment', *IEEE Trans. Image Proces.*, 2006, **15**, (2), pp. 422–429
18 Narwaria, M., Lin, W.S.: 'Scalable image quality assessment based on structural vectors'. IEEE Int. Workshop on Multimedia Signal Processing, Rio de Janeiro, Brazil, 2009, pp. 1–6
19 Narwaria, M., Lin, W.S.: 'Objective image quality assessment based on support vector regression', *IEEE Trans. Neural Netw.*, 2010, **21**, (3), pp. 515–519
20 Han, H.S., Kim, D.O., Park, R.H.: 'Structural information-based image quality assessment using LU factorization', *IEEE Trans. Consumer Electron*, 2009, **55**, (1), pp. 165–171
21 Kim, D.O., Han, H.S., Park, R.H.: 'Gradient information-based image quality metric', *IEEE Trans. Consumer Electron*, 2010, **56**, (2), pp. 930–936
22 Zhu, J.Y., Wang, N.C.: 'Image quality assessment by visual gradient similarity', *IEEE Trans. Image Process.*, 2012, **21**, (3), pp. 919–933
23 Aja-Fernandez, S., San Jose Estepar, R., Lopez, C.A., *et al.*: 'Image quality assessment based on local variance'. IEEE Int Conf. Engineering in Medicine and Biology Society, New York City, 2006, pp. 4815–4818
24 Sheikh, H.R., Sabir, M.F., Bovik, A.C.: 'A statistical evaluation of recent full reference image quality assessment algorithms', *IEEE Trans. Image Process.*, 2006, **15**, (11), pp. 3440–3451
25 Angelis, A.D., Moschitta, A., Russo, F., *et al.*: 'A vector approach for image quality assessment and some metrological considerations', *IEEE Trans. Instrum. Meas.*, 2009, **58**, (1), pp. 14–25
26 Russo, F., De Angelis, A., Carbone, P.: 'A vector approach to quality assessment of color images'. IEEE Int. Conf. on Instrumentation and Measurement Technology, Vancouver Island, Canada, 2008, pp. 814–818
27 Targhi, A.T., Shademan, A.: 'Clustering of singular value decomposition of image data with applications to texture classification', *Proc. SPIE*, 2003, **5150**, pp. 972–979
28 VQEG: 'Final report from the video quality experts group on the validation of objective models of video quality assessment phase II' (Video Quality Experts Group, 2003)